Probing the paramagnetic interactions between the unpaired electronic spins of carbon atoms and the nuclear spins of hydrogen molecules with Raman spectroscopy

Andrea Centrone[1,2,3*]

1 Politecnico di Milano, Dipartimento di Chimica, Materiali e Ingegneria Chimica "Giulio Natta" 20133 Milano, Italy

2 NIST, Center for Nanoscale Science and Technology, Gaithersburg, 100 Bureau Drive, Stop 6204, MD 20899, USA.

3 University of Maryland, Institute for Research in Electronics and Applied Physics, College Park, MD 20742, USA

Abstract

Carbon materials typically have a high density of unpaired electronic spins but the exact nature of the defect sites that give rise to their magnetic properties are not yet well understood. In this work, the paramagnetic interactions between the unpaired electronic spins of carbon atoms and the nuclear spins of hydrogen molecules were probed with Raman spectroscopy by monitoring the relative population of H_2 rotational states. For H_2, the symmetries of nuclear spin and rotational wave functions are correlated. Because of the weak interactions between H_2 nuclear spins, the transitions between odd and even rotational states are normally hindered. The magnetic field generated by unpaired electronic spins relaxes the selection rules and promotes transitions between H_2 rotational levels of different symmetry. This affects the rotational levels relaxation kinetics toward equilibrium and makes H_2 molecules useful to study unpaired electrons in paramagnetic materials. It is suggested that simultaneous EPR and Raman measures on carbon materials interacting with hydrogen molecules could result in a better understanding of the nature of paramagnetic defects in carbon materials, which could have a substantial impact on Li-ion batteries or for understanding the graphene electronic properties.

Keywords: *Raman Spectroscopy, paramagnetic properties, spin, intermolecular interactions, carbon materials.*

* Corresponding author. Tel.: +1 301-9758225. E-mail address: andrea.centrone@nist.gov (A. Centrone)

Introduction

Carbon materials ranging from amorphous carbon (AC) to nanotubes (CNT) and ultimately to graphene have attracted attention for their application in surface coatings,[1] electronics,[2] Li-ion batteries,[3] and hydrogen storage,[4, 5] to name a few. Carbon materials have high densities of unpaired electronic spin (10^{17} g^{-1} to 10^{21} g^{-1})[6, 7] but the exact nature of the defect sites that give rise to their magnetic properties are not yet well understood. Contrary to the chemical intuition which attributes to dangling bonds a high reactivity, radicals in carbon materials can be quite stable.[8] Stabilization by delocalization of π unpaired electrons has been suggested in early literature,[9, 10] while recently, stabilization by localization of itinerant π electrons in unsatured zig-zag or armchair edge sites, was proposed.[8] The localization of the dangling bonds in zig-zag sites was suggested to be responsible for most of the magnetic properties in carbons.[8, 11] While Raman spectroscopy was recently used to study van Der Waals interactions between adsorbed hydrogen molecules and porous materials,[5, 12] in this work, the Raman spectra were used to study the paramagnetic interactions occurring between H_2 nuclear spins and carbon radicals and show that H_2 molecules can be used to probe the paramagnetic properties of carbon materials. The author believes that the method described here will stimulate research on carbons' paramagnetic properties and ultimately could result in better understanding of these materials in applications such as Li-ion batteries and electronics.

Experimental

A commercial AC material (Norit CASPF)† and a carbon material obtained by pyrolyzing Hexa-Phenyl Benzene (HPB) precursor molecules at 550 °C for 3 days (TR21B)[13] were analyzed in this work. At 82 K TR21B and AC adsorb a H_2 mass fraction of 0.6 % and 2.25 %,[5]

† The materials used in this paper require the identification of a commercial product and its supplier. The inclusion of such information should in no way be constructed as indicating that such product or supplier is endorsed by NIST or is recommended by NIST or that is necessarily the best material for the purpose described

respectively. TR21B is composed by a mixture of two-dimensional polycyclic aromatic hydrocarbon (PAH) sheets with peculiar features ("holes") strictly related to the precursor molecules chemical structure, Fig. S1 (Supporting Information).[3, 13] With respect to an ideal graphitic plane those "holes" can be described as six missing carbon atoms; while six hydrogen atoms saturate the adjacent carbon atoms.[13] The edge profiles of these *holes* are neither armchair nor zig-zag.

A spectrometer in double subtracting configuration was used to record the Raman spectra using a 514.5 nm exciting line (Ar ion, 25 mW) with a spectral resolution of 1.2 cm^{-1}. The Raman spectra were collected is situ using a custom made cell attached to a cold finger of a helium cryostat as described previously.[13] An achromatic lens (focal length 7.5 mm, NA 0.27) was used to focalize the laser beam (spot size ≈ 1 mm) inside the cell in the gas phase and not on the carbon sample. It is reasonable to assume that the H_2 temperature is roughly unaffected by the measure because of the large laser spot size and the relative large density of H_2 at 40 K and 0.81 MPa, which makes the heat transfer process quite efficient. The samples were degassed overnight in high vacuum ($1 \cdot 10^{-10}$ MPa ± $0.1 \cdot 10^{-10}$ MPa) in situ at 298 K before introducing H_2 (0.81 MPa ± 0.1 MPa) into the cell. The Raman spectra were recorded as a function of time at 40 K ± 1 K by averaging 4 spectra (20 s each) for each sample. The integration of the sharp H_2 Raman lines was carried out without smoothing.

Electron-Paramagnetic Resonance (EPR) experiments were recorded at room temperature and the radical density was evaluated with Bruker weak pitch standard.

Results and Discussion

The H_2 total wave function (Ψ) is symmetric and, assuming independent the degrees of freedom of the molecule, can be written as the product of the nuclear spin, electronic, vibrational

and rotational wave functions ($\Psi = \Psi_{Nspin} \cdot \Psi_{elet} \cdot \Psi_{vibr} \cdot \Psi_{rot}$). In the fundamental energy level Ψ_{elet} is symmetric while Ψ_{vibr} is always symmetric; consequently, Ψ_{Nspin} and Ψ_{rot} must have the same symmetry. Hydrogen molecules in odd rotational states have parallel nuclear spins (↑↑) and antisymmetric Ψ_{rot}; vice versa, hydrogen molecules in even rotational states have antiparallel nuclear spins (↑↓) and symmetric Ψ_{rot} (Fig. 1a).[14] For homonuclear molecules whose atoms have non zero nuclear spin (i.e. H_2) the transition between odd and even rotatiotional states is not strictly forbidden because it preserves the Ψ symmetry, but it is improbable because of the small spins' magnetic moment and their consequent weak interaction. In other words, the transition probability between two rotational states of different symmetries (but with the same symmetry of the total wave function Ψ) is not exactly zero but close to it. Practically, H_2 consist of a mixture of two gases, one that "lives" in the even rotational states (*para hydrogen*) and one that "lives" in the odd rotational states (*ortho hydrogen*); for this reason H_2, is often out of thermodynamic equilibrium. At low temperature, the first rotational level (J=1) can hardly be depleted because of the slow kinetics of the *ortho-para* transitions (ΔJ=-1). The inhomogeneous magnetic field of unpaired electrons catalyzes the H_2 *ortho-para* transitions, thus accelerating the establishment of the equilibrium;[15, 16] the stronger the interaction the larger is the transition probability.

The *ortho-para* relative populations can be quantified integrating the areas of the H_2 Raman lines. At room temperature the *ortho-para* ratio (*r*) at equilibrium is 3, reflecting the multiplicity of the nuclear statistics; while at 40 K *r* should be 0.033. The Raman spectra in figure 1b (0.81 MPa, 40 K) clearly show that the interaction with the AC catalyzes the *ortho-para* conversion but even after 166 h the thermodynamic equilibrium could not be established. The evolution of the hydrogen *ortho-para* ratio as a function of time at 40 K is reported in figure 2 for natural

decay, for the interaction with AC (5.8 mg), and with TR21B (7.5 mg). The experimental data can be fitted with a simple exponential function: $r(t) = r_0 \cdot e^{-kt}$ where r_0=3 is the initial *ortho-para* ratio and *k* is a constant which depends on the molar ratio between hydrogen molecules and the carbon radicals on the material surface; *k* also depends on the temperature which affects the absorption/desorption kinetics. At low temperature the *ortho-para* conversion is limited by the hydrogen desorption rate.[15] Adsorbed hydrogen molecules reach relatively quickly the thermodynamic equilibrium but the slow desorption kinetics at 40 K makes the establishment of the equilibrium in the gas phase difficult. The H_2 half-life was ≈ 578 h for natural decay while the interaction with the TR21B and AC decreased the half-life to ≈ 192 h and ≈ 58 h, respectively. These experiments raise the question whether the amount and/or the nature of the paramagnetic defects on these two carbon materials is different (i.e. localized differently).

The EPR signals (Fig. 3) of the analyzed samples are isotropic with a *g* value of 2.0025. TR21B has larger unpaired electronic spin density ($3.24 \cdot 10^{19}$ g^{-1}) and narrower EPR line width (1.47 mT) than the AC sample ($6.05 \cdot 10^{18}$ g^{-1}, 17.0 mT). The absolute error of the number of radicals is in the order of 20 % but the relative error for the 2 samples, analyzed with the same instrumental parameters, is much smaller. Even if AC has a smaller radical density, it is more efficient in catalyzing the ortho-para conversion (Fig. 2). AC adsorbs more H_2 than TR21B[[5]] and, normalizing for the differences in adsorbed H_2, weight and radical density, TR21B is expected to be twice more effective in catalyzing the *ortho-para* conversion than AC, in contradiction with the experimental observations (AC is 10 times more effective after normalization). Either the radicals found in TR21B are less effective, e. g. more localized, in catalyzing the *ortho-para* transition or most of them are embedded in the material and don't interact with the gas.

Pyrolyzed materials like TR21B showed very large lithium uptake;[3] additionally, theoretical calculations[17] showed that Li binds preferentially to PAH's edges. Carbon radical defects, probably localized at zig-zag edge sites of carbon materials, could be relevant for lithium uptake and could have a substantial impact on Li-ion batteries or on graphene electronic properties. The author believes that this work will stimulate further research to better understand the nature of paramagnetic defects in carbon materials. Conducting simultaneous in situ EPR and Raman measures on structurally defined and homogeneous materials like CNTs, graphene or PAHs offers the opportunity to improve our understanding of carbon radicals in these materials. It is proposed to conduct such experiments at room temperature using *para* enriched H_2 to substantially speed up the conversion rates of the *para-ortho* transitions and the achievement of the equilibrium.

Acknowledgements This work was supported by the European Commission, 5th Framework Programme (G5RD-CT2001-00571). The author thanks Prof. Giuseppe Zerbi for the fruitful discussions and Prof. Roberto Scotti for the EPR measures.

[1] S. Neuville, A. Matthews, *Thin Solid Films* **2007**, *515*, 6619.
[2] V. Sgobba, D. M. Guldi, *Chem. Soc. Rev.* **2009**, *38*, 165.
[3] T. Renouard, L. Gherghel, M. Wachtler, F. Bonino, B. Scrosati, R. Nuffer, C. Mathis, K. Müllen, *J. Power Sources* **2005**, *239*, 242.
[4] B. Panella, M. Hirscher, S. Roth, *Carbon* **2005**, *43*, 2209.
[5] A. Centrone, L. Brambilla, G. Zerbi, *Phys. Rev. B* **2005**, *71*.
[6] R. C. Barklie, *Diamond Relat. Mater.* **2001**, *10*, 174.
[7] H. J. von Bardeleben, J. L. Cantin, K. Zellama, A. Zeinert, *Diamond Relat. Mater.* **2003**, *12*, 124.
[8] L. R. Radovic, B. Bockrath, *J. Am. Chem. Soc.* **2005**, *127*, 5917.
[9] S. E. Stein, *Acc. Chem. Res.* **1991**, *24*, 350.
[10] S. E. Stein, R. L. Brown, *J. Am. Chem. Soc.* **1991**, *113*, 787.
[11] K. Nakada, M. Fujita, G. Dresselhaus, M. S. Dresselhaus, *Phys. Rev. B* **1996**, *54*, 17954.
[12] A. Centrone, D. Y. Siberio-Perez, A. R. Millward, O. M. Yaghi, A. J. Matzger, G. Zerbi, *Chem. Phys. Lett.* **2005**, *411*, 516.
[13] A. Centrone, L. Brambilla, T. Renouard, L. Gherghel, C. Mathis, K. Mullen, G. Zerbi, *Carbon* **2005**, *43*, 1593.
[14] G. Herzberg, *Spectra of Diatomic molecules, Vol. 1*, New York, **1950**.
[15] L. Farkas, L. Sandler, *J. Chem. Phys.* **1940**, *8*, 248.
[16] K. F. Bonhoeffer, P. Harteck, *Z. Phys. Chem. B* **1929**, *4*, 113.
[17] G. Brancolini, F. Negri, *Carbon* **2004**, *42*, 1001.

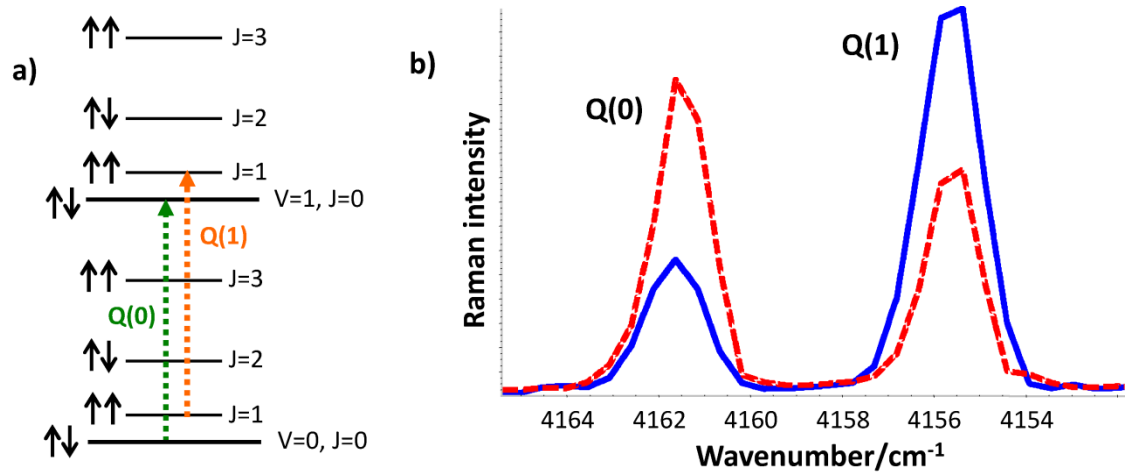

Fig. 1: a) Schematic of H_2 vibro-rotational energy levels. b) H_2 Raman spectra at 40 K: initial (solid line) and after 166 h of interaction with AC (dotted line). The Q branch selection rules are $\Delta v = +1$ and $\Delta J = 0$. The first rotational level (J = 1) is initially more populated than the fundamental level (J = 0).

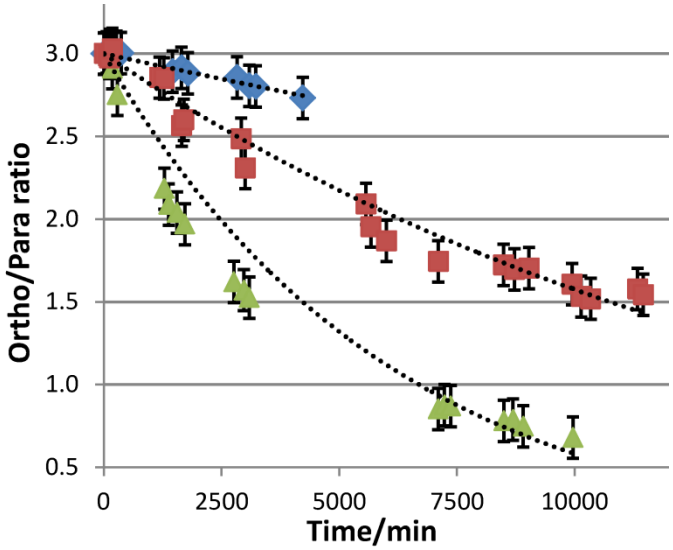

Fig. 2: At 40 K the hydrogen *ortho-para* ratio (r) decays exponentially as a function of time ($r(t) = 3 \cdot e^{-kt}$), for natural decay (diamonds, $k = 2.09 \cdot 10^{-5}$ s^{-1}, $R^2 = 0.97$); for H_2 interacting with AC (triangles, $k = 1.64 \cdot 10^{-4}$ s^{-1}, $R^2 = 0.96$) and for H_2 interacting with TR21B (squares, $k = 6.45 \cdot 10^{-5}$ s^{-1}, $R^2 = 0.97$). The error bars represent a single standard deviation in the integration of the Raman lines.

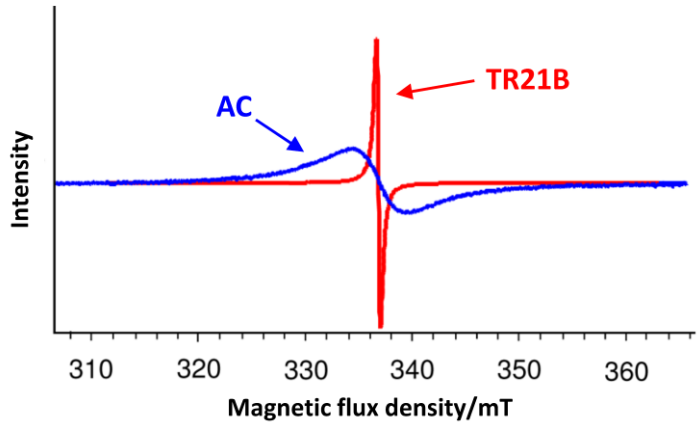

Fig. 3: EPR spectra of AC (blue) and TR21B (red).

Supporting information

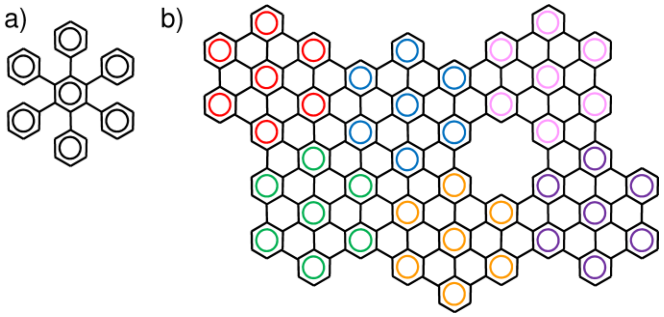

Fig. S1: a) Hexa-phenyl-benzene (HPB). b) PHA model molecule obtained by the HPB pyrolysis. The materials obtained by the pyrolysis of HPB are composed by PAHs mixtures.[13] Statistically the pyrolysis of HPB is likely to generate defects, where, 6 carbons are missing.[13] The colours of PAH model molecule are just to indicate the individual precursor molecules from which it derives.